Climate Dynamics (1998) 14: 529–536

T. Schmith · E. Kaas · T.-S. Li

Northeast Atlantic winter storminess 1875–1995 re-analysed

Received: 20 May 1997 / Accepted: 13 January 1998

Abstract Northeast Atlantic winter storminess is analysed for the period 1875–1995 using a new dataset consisting of multi-daily mean sea level pressure observations from a selected set of stations in the northeast Atlantic. An analysis of storminess is presented, based on the high-pass filtered signal from these observations, from which selected percentiles are calculated for each winter. This method avoids potential inhomogeneity problems (artificial trends or jumps). Our finding is an increase, however not a dramatic one, during the past 2–3 decades in the northeasternmost part of the storm track, but the dominant features are inter-annual and decadal variations. Furthermore, the variations in storminess are found to be statistically linked to low-frequency circulation variations represented by the winter average of the MSL pressure field over the North Atlantic. It is argued that the existence of this link could have dynamical consequences for the response of the atmosphere to external forcing.

1 Introduction

In the ongoing world debate about climatic changes and possible human influences, the public has from time to time been alarmed by bulletins coming from widely different sectors of the society such as insurance (Berz and Conrad 1994), offshore industry and non-governmental organisations (Greenpeace 1994). Postulated recent increase in frequency of meteorological phenomena such as tropical hurricanes, wind storms or storm surges are taken as signs of the weather becoming more extreme. These messages often find their way to newspaper headlines and therefore have great impact on politicians and public opinion. However, they seem problematic, based as they are on rumours, subjective and inhomogeneous quantities such as 'insurance losses' etc. and most often taking only the latest 5–10 y into account.

The question of trends in storminess in the North Atlantic region may at a first glance seem trivial as wind observations have been made on a routine basis since the second half of the last century. We argue that these wind data are, however, essentially unusable as means to detect rather small trends, since the data are subject to changes in observational procedure and to changes in instruments and their surroundings. Within the climatological community this type of time series is regarded as *inhomogeneous* (Conrad and Pollack 1962). Avoiding inhomogeneities was of decisive importance in our choice of analysis method. Another difficulty when detecting a trend is related to the length of the observational record which must be long enough so that the trend is not severely masked by natural climatic variability.

At this point it may be appropriate to consider the implications *if* a trend in storminess were to be detected. Recent published model simulations of increasing CO_2-content of the troposphere (Carnell et al. 1996; Lunkheit et al. 1997) suggest an intensification and eastward extension of the Atlantic storm track, i.e. more storm activity in the northeast Atlantic/northwestern Europe, in the $2 \times CO_2$ case compared to present-day conditions. This, however, does not prove, that an observed increase in this area is caused by increased

T. Schmith (✉) E. Kaas · T.-S. Li[1]
Danish Meteorological Institute,
Climate Research Division,
Lyngbyvej 100, DK-2100 København Ø, Denmark
E-mail:tsc@dmi.dk

Present address:
[1]Iowa State University,
Department of Geological and Atmospheric Sciences,
3018 Agronomy Hall, Ames, IA 50011,
USA

This paper was presented at the European Geophysical Society General Assembly, Vienna, 21.–25. April 1997

greenhouse effect. Changes in storminess are interlinked with changes in the general three-dimensional structure of the atmosphere and such changes may just as well be manifestations of internal variability in the coupled atmosphere-ocean system. Therefore, our analysis cannot in any way, point to the underlying reasons for an observed trend.

Section 2 contains a review and discussion of earlier investigations on the subject. Section 3 is a short description of the data and method used. In Sect. 4 the analysis of storminess is presented, and in Sect. 5 variations in storminess are related to variations in the background state by a statistical hindcast model. In Sect. 6 dynamical interpretation of the statistical model is given and in Sect. 7 the implication of the statistical link is discussed further. The findings from the previous sections are given in the concluding Sect. 8.

2 Earlier investigations of storminess in the North Atlantic

Several investigations have been published on storm frequency in the North Atlantic region based on historical weather maps. Schinke (1993) investigated the annual number of lows from 1930–1991 and found distinct temporal variations in the cyclone frequency with a particularly distinct rise starting in the early 1970s. Stein and Hense (1994) investigated the number of lows during winter (November–March) 1890–1993 and also found a large interannual variability in the number of extreme lows. Their analysis revealed that the years around 1970 were very quiet, followed by an extraordinary upward trend. In particular winters since 1988/89 show a number of extreme lows never recorded before. Lambert (1996) studied winter cyclone events 1899–1991 and found little trend in the number of intense lows before 1970 but a sharp increase after 1970.

However, the methodology of such investigations has been criticised for being inhomogeneous by von Storch et al. (1993). They point out that over the last 100 years the number of merchant ships crossing the Atlantic has increased. After the World War II about 10 ocean weather ships were stationed in selected positions throughout the North Atlantic for a long period. These ships were later withdrawn, but in the 1960s weather satellites and numerical models of gradually improving resolution and quality were introduced. Thus there is possibly a tendency to catch deeper and deeper lows in the analyses, which were simply unsampled in earlier times, but may still have been present. In other words, the extreme values of the pressure are inhomegeneous. Note that such inhomogeneities will not be found in Trenberth and Paolino (1980), where the monthly *mean* pressure data from a widely used historical gridded dataset are tested and found mainly homogeneous over the North Atlantic.

Historical records of wind observations are subject to similar severe inhomogeneities and are not usable for detecting trends. First of all instrumental measurement of the wind did not begin until the 1950s. Before that time wind observations were based on subjective judgement of the wind force by observers, using the Beaufort scale, however without any universally agreed standard. Also the instrumentally based winds from the 1950s onwards are inhomogeneous due to replacement of old instruments by more modern ones and by changes in the immediate surroundings of the measuring site due to growing and cutting of trees etc. In practice it is impossible to keep track of, not to mention correct for, all these changes (Cardone and Greenwood 1990) and therefore the literature contains hardly any analyses of historical wind series over a 100 year period.

Schmidt and von Storch (1993) avoided inhomogeneity problems by investigating the *geostrophic* wind climate in an area in the southeastern North Sea. According to this work, the geostrophic wind can be taken as a proxy for the real wind and is proportional to the strength of the horizontal pressure gradient. It can therefore be calculated from pressure observations only. Pressure observations are believed to be fairly homogeneous, as they are almost independent of observer and instrument. In their work the authors calculated the pressure gradient from pressure observations reduced to mean sea level from three stations separated by around 150 km and found no increase in geostrophic storminess but rather a remarkable constancy over more than 100 years.

The geostrophic triangle method has been extended to the northeast Atlantic and Scandinavia by Alexandersson et al. (1997), whose main findings were a slow decrease in annual storminess from 1880 to about 1960 and from around 1970 an increase (in particular in the northeast Atlantic) to levels at or above pre-1900 levels. The picture found in Schinke (1993), Stein and Hense (1994) and Lambert (1996) was thus in many respects confirmed, although the winters around 1990 were found not to be so extreme.

3 Method and data

The present work is based on pressure observations due to the reasons discussed in the previous section. However, the geostrophic wind approach could be questioned for the following reasons:

1. The Rossby radius of deformation for the atmosphere is of the order of 1000 km, which is also the scale of an extratropical low. Therefore, when resolving the wind on smaller scales, the ageostrophic effect may be important, i.e. the geostrophic wind may not be a proxy for the real wind.
2. Different stations sometimes have different observation hours. Therefore interpolation in time is needed which lead to uncertainties and potential inhomogeneities (Schmith et al. 1997).
3. Inhomogeneities in the pressure series will be directly reflected in the geostrophic winds.

To overcome these problems we have used high-pass filtered MSL pressure as a measure of cyclonic activity, see Wallace et al. (1988)

Table 1 Names and positions of the eight stations selected for the investigation

Number	Station	Latitude	Longitude
1	Ammassalik	65°36′N	37°38′W
2	Jan Mayen	70°56′N	8°40′W
3	Stykkisholmur	65°05′N	22°44′W
4	Torshavn	62°01′N	6°46′W
5	Aberdeen	57°10′N	2°06′W
6	Valentia	51°56′N	10°15′W
7	Bodø	67°16′N	14°26′E
8	Bergen	60°23′N	5°20′E

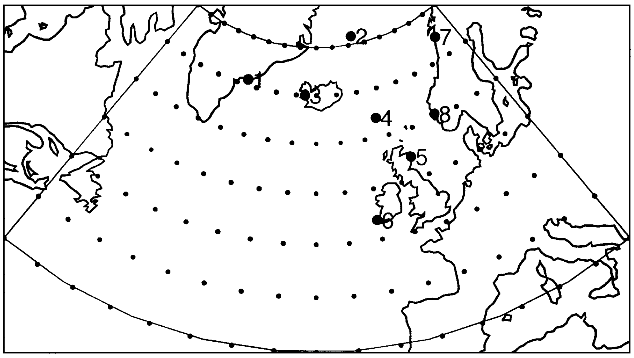

Fig. 1 Map showing the geographical domain of interest. Positions of the eight stations selected for the investigation are marked with *large dots*. Gridpoints with monthly mean MSL pressure values used in the statistical hindcast model marked by *small dots*

for a discussion of this measure. In our case, we applied a very simple high-pass filter, namely the absolute value of the pressure tendency, i.e. the change in atmospheric pressure during a given time span. From synoptic experience this quantity is known to be connected to cyclonic activity and is also discussed in Kaas et al. (1996).

The data, on which we base our investigation, consist of pressure observations from eight carefully selected stations in the northeast Atlantic. The main selection criteria are a long and unbroken observation record, preferably ranging back to the latter part of the nineteenth century with 3–4 daily observations. A good spatial coverage is also important. Details about the selected stations are given in Table 1 and geographical locations are shown in Fig. 1. Pressure data from these stations have been digitised and manual quality control of extreme values was widely applied. The data is part of a larger dataset published in Schmith et al. (1997).

Some of these stations have observation hours which are not equally-spaced over the day and in some cases not even constant over the period. Therefore 24-hour tendencies were calculated, i.e. the absolute 24-hour change in pressure. This corresponds to applying a bandpass filter with 100% transfer at 48 h and 50% transfer at 84 h and 32 h.

As the majority of storms occur during winter time the following analysis is confined to the months December, January and February, giving a stastistical basis of about 300 observations per winter.

4 Results

Not only the study of mean values of 'storminess', but rather the entire distribution of the pressure tendencies for each winter is of interest. One easy way to get an overview of this distribution is to consider the *exceedance levels*, defined as the lower bound of the x% highest absolute pressure tendencies. In this analysis three standard levels 50%, 10% and 1% will be considered. Since each winter's length is approximately 2000 h, these three standard exceedance levels are, on the average, each winter exceeded approximately 1000 h, 200 h and 20 h respectively.

The three standard exceedance levels are plotted against year in Fig. 2. The most noticeable feature for all stations is the large inter-annual variations, but also considerable variations on decadal time scale are present. This is emphasised by the low-pass filtered curves also present in Fig. 2.

The main features of the storminess for each station are as follows: Ammassalik shows decreasing storminess until around 1940 followed by a rather constant level. Jan Mayen's shorter record has a relatively constant level throughout the period. Stykkisholmur's storminess shows a steep increase until around 1900 followed by an abrupt decrease and thereafter a rather constant behaviour. Torshavn shows constant behaviour after about 1900 until around 1970, after which a steady increase occurs. Aberdeen has a constant level followed by a decrease after 1900 until around 1920, from when the storminess rate is fairly constant. Valentia is the only station that shows an increase throughout the century. Bodø shows a constant level until around 1970, followed by an increase. The same description holds for Bergen.

Thus the temporal changes of storminess are different at the individual stations, and any common trend or variation is hard to detect. The most remarkable feature is the 15–20% increase in storminess seen since around 1970 observed at Torshavn. This increase is also reflected in the Bodø and Bergen records but, surprisingly, not in the Aberdeen record.

5 Relation between storminess and mean circulation

The interdependence between changes in the cyclone track and low frequency variability of the atmospheric state has been subject to several empirical studies, e.g. Lau (1988) based on the 500 hPa height field. We wanted to carry out a similar analysis. However, only MSL fields are available dating back to the previous century. Thus the mean monthly MSL pressure field has been used to represent the large-scale atmospheric state in the following section.

The method applied was a multilinear regression technique applied to each station separately, where the storminess exceedance levels for each winter (the predictand) were linked to winter means of the mean MSL pressure field from the area 40°N–70°N and 60°W–20°E (predictor field, area indicated on Fig. 1). These latter data were available on a 5 × 5 degree grid

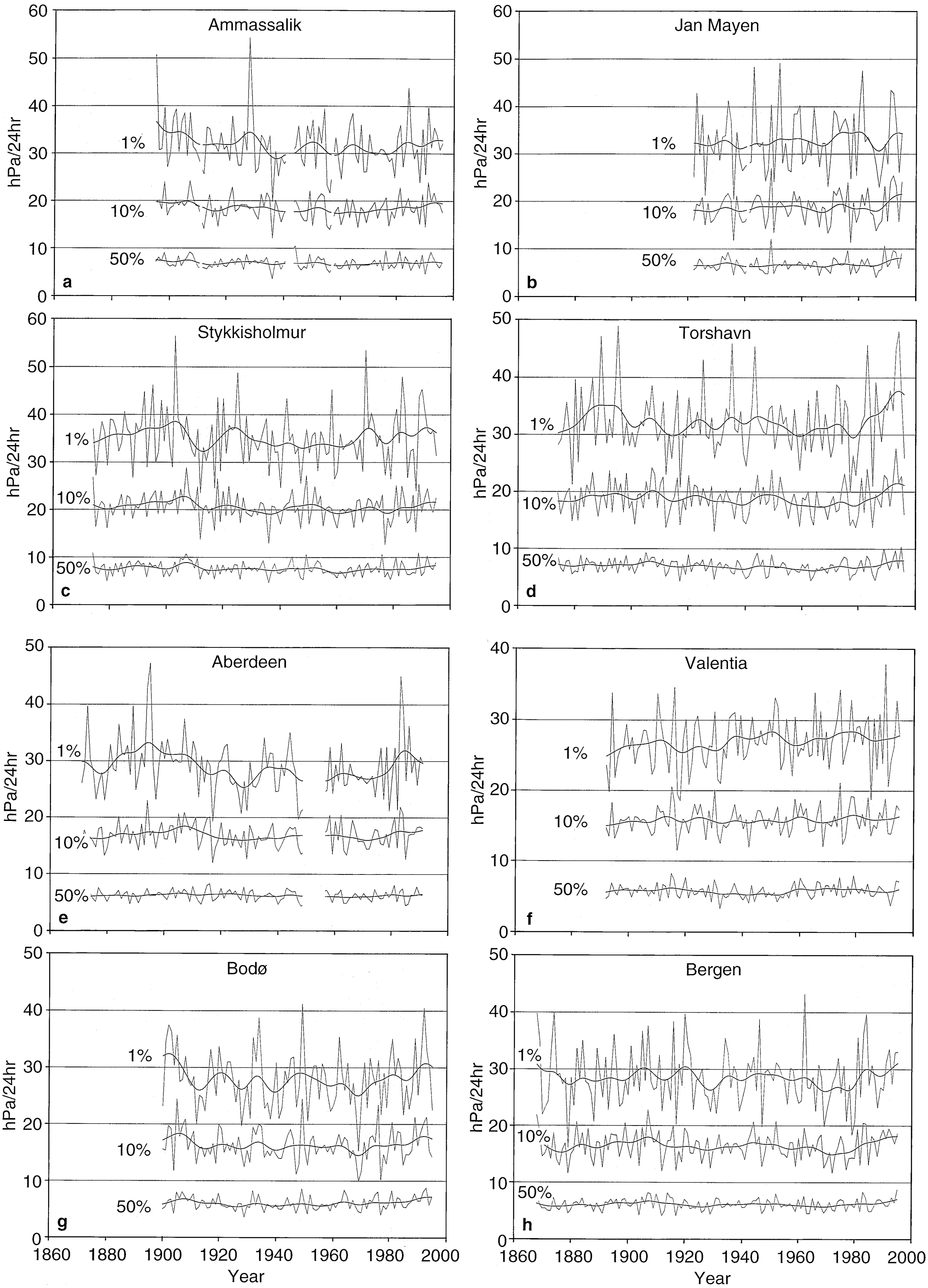

Fig. 2a–h Plots showing the three standard exceedance levels for each winter (DJF) for the eight stations. The *thick curves* are obtained by applying a Gauss-filter with a standard deviation of 3 y, corresponding approximately to a running mean with 10 y window length

for the winters 1900–1995 from NCAR as dataset ds010.1 (Trenberth and Paolino 1980).

To avoid intercorrelations a filtering of the predictor field was performed, based on standard EOF-decomposition. The time series of coefficients in this expansion are called principal components (PCs), $\alpha_i(t)$, and are found by projecting the mean pressure anomaly field for each winter, $p'(\vec{r}, t)$ onto the EOFs, $e_i(\vec{r})$. In order to minimise noise, only the first 4 PCs (corresponding to the most significant EOFs), explaining 85% of the variance, were retained. Mathematically, we have

$$p'(\vec{r}, t) = \sum_{i=1}^{4} \alpha_i(t) \cdot e_i(\vec{r}) \quad (1)$$

The most significant EOF explains 41% of variance and is a pattern connected to the North Atlantic Oscillation (NAO) index (Walker and Bliss 1932).

The 4 PCs were then used as predictors in the statistical model. This model for one of the three standard exceedance levels, χ, mathematically may be written as

$$\chi(t) = \bar{\chi} + \sum_{i=1}^{4} b_i \cdot \alpha_i(t) \quad (2)$$

where $\bar{\chi}$ is the time-average of the exceedance level and b_i is the coeffficient determined in the regression analysis. The model was used in connection with a cross-validation technique so that when hindcasting a particular year, the predictors from that year and from the neighbouring years was omitted. This is in order to base the hindcast on independent data. The entire model is very similar to the one used in our earlier work (Kaas et al. 1996).

The correlation coefficients between hindcast and observed values are shown in Table 2 for all 8 stations. The 50% level values have the highest values (0.66–0.82), but the 10% level values are hindcast with almost as good a performance (0.61–0.74). In contrast, the 1% level values are hindcast with somewhat poorer performance (0.34–0.55). The highest values of the correlation coefficient are found for the stations Stykkisholmur and Torshavn, which are both close to the North Atlantic storm track. As an example, the observed and hindcast time series for Torshavn are shown in Fig. 3, which shows that the model reproduces the observed values quite well. In particular we note that the increase in storminess from around 1980 can be explained by the model to a large extent.

Table 2 Correlation coefficients between observed and hindcast time series for the selected stations and for the three standard exceedance levels, calculated on *independent* data as explained in the text

Number	Station	Correlation coefficient		
		50%	10%	1%
1	Ammassalik	0.74	0.68	0.34
2	Jan Mayen	0.74	0.70	0.48
3	Stykkisholmur	0.82	0.72	0.41
4	Torshavn	0.80	0.73	0.48
5	Aberdeen	0.66	0.65	0.48
6	Valentia	0.66	0.61	0.45
7	Bodø	0.76	0.74	0.55
8	Bergen	0.70	0.68	0.54

6 Optimal predictor maps

In order to increase our physical understanding of the hindcast model, *optimal predictor maps* (OPMs) have been introduced, see also Kaas et al. (1996). Using the OPM is an alternative way of formulating the hindcasting model. The OPM itself has a very simple interpretation, it is the predictor pattern which results in one standard deviation increase in the predictand. A technical description of calculating OPMs is in the Appendix.

We found that the OPMs corresponding to one station (one for each exceedance level) are very similar. This is quite satisfying, since it supports the idea that the entire distribution of the pressure tendency is a manifestation of a general process, namely variations in the general structure of the atmosphere. Furthermore, OPMs for neigbouring stations are also similar. As an example, OPMs for the 10% exceedance level for the stations Torshavn and Bergen are shown in Fig. 4.

For the stations Stykkisholmur, Torshavn, Bodø and Bergen the OPMs have similarities: they are all bipolar structures with a negative pole over northwestern Scandinavia and a positive pole in the Biscay area. That means that the patterns associated with storminess in the northeastern Atlantic are significantly different from the NAO pattern. The reason for that is not known, but the finding is in agreement with Rogers (1997). Stations Aberdeen and Valentia have somewhat different patterns: the negative pole is shifted towards southwest. For stations Ammassalik and Jan Mayen the negative pole is displaced towards Greenland.

7 Further discussion of statistical model

A suitable framework for discussing extratropical cyclonic activity is the simplified Eady-wave theory by Lindzen and Farrel (1980). According to this, the e-folding time of the fastest growing wave σ_{max}, is given by

$$\sigma_{max} = 0.3125 \times \frac{f}{N}\frac{du}{dz} = -0.3125 \times \frac{R}{N}\nabla T \quad (3)$$

where we have used the thermal wind relation in the last transcription. In these equations f is the Coriolis parameter, R is the gas constant for atmospheric air, N is the Brunt-Väisälä frequency, u is the zonal wind

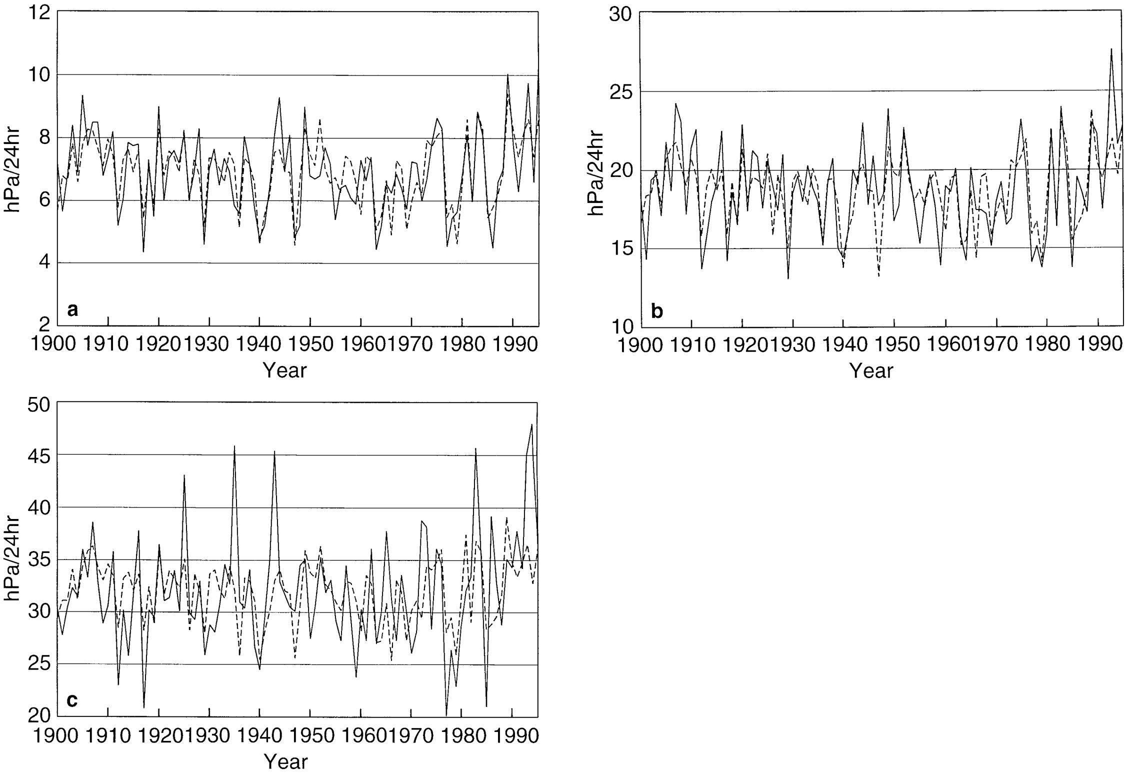

Fig. 3a–c Plots of observed (*solid curve*) and hindcast (*dashed curve*) standard exceedance levels **a** 50%, **b** 10% and **c** 1% of the absolute pressure tendencies for each winter 1900–1994 for station 4: Torshavn. Note the *different ordinate axes* on the three sub-plots

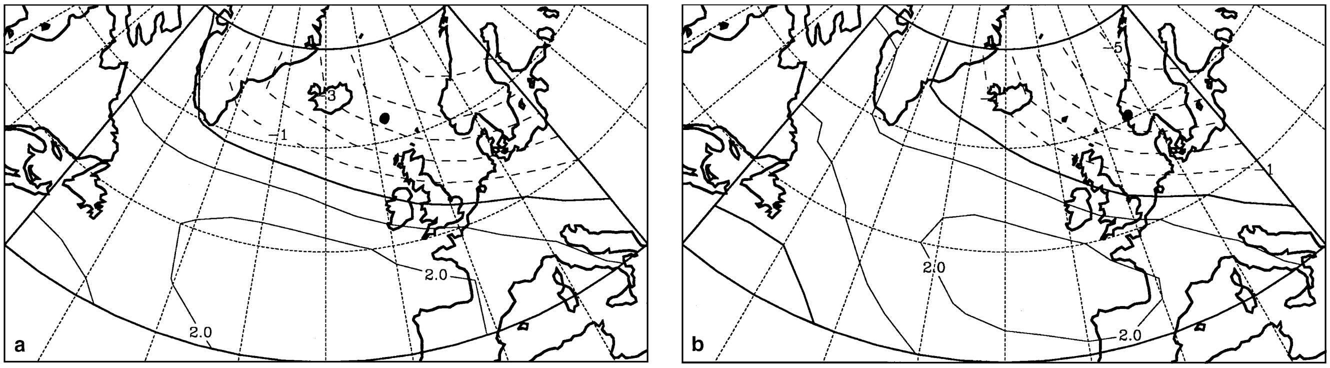

Fig. 4a–b OPM corresponding to the 10% exceedance level for the stations **a** Torshavn and **b** Bergen. Contour interval is 1hPa and negative coentours are *stipled*

and ∇T is the meridional temperature gradient (all calculated from the basic state). Hoskins and Valdes (1990) showed that σ_{max} calculated from winter climatological fields reproduced the observed storm track quite well and Hall et al. (1994) and Lunkeit et al. (1996) used σ_{max} for estimating changes in storm tracks in CO_2 scenario experiments.

The synoptic activity is therefore expected to be determined by ∇T and N. Thus, in relation to our statistical model we have two possibilities: (a) N and ∇T are given entirely by the MSL pressure field, in which case the residual time series, i.e. the time series of hindcast values subtracted from the time series of observed values, is a realisation of a white noise process, or (b) N and ∇T not uniquely given by the MSL pressure field, but other predictors are neccesary. For instance, CO_2-enhanced greenhouse effect may have changed N systematically throughout the century. In the latter case the residual time series is not a realisation of a white noise process.

The test for case (a) versus (b) is made by applying the white noise test described in Jenkins and Watts (1968). In this test also significance levels, based on the Kolmogorov-Smirnov test are given. We applied this test to all our 8×3 residual time series and found all these to be consistent with realisations of white noise processes at the 95% significance level.

The statistical test of the residual time series shows an advantage for case (a). This does *not* exclude any external forcing of the atmosphere, but indicates that the relations between synoptic and larger scales are very robust and therefore likely to be unchanged under different forcings of the atmosphere.

8 Conclusions

By applying a commonly used high-pass filter to pressure data in multi-daily temporal resolution from eight stations in the northeast Atlantic a homogeneous representation of the storminess in the area during the period 1875–1995 has been obtained.

From the analysis it is evident that some increase in storminess has taken place during the past 2–3 decades in the northeast Atlantic storm track. These results cannot be compared directly to earlier investigations based on historical weathermaps, however, it seems likely that some of these latter investigations are affected by inhomogeneities, in particular around 1990.

Furthermore, the variations in storminess have been shown to be statistically linked to low-frequency variations in the atmospheric circulation in a robust manner, that remains the same over the entire period of investigation. This has an important consequence for the atmospheric dynamics, because it implies that *if* changes in forcing with impacts on storminess have occurred, these have not manifested themselves directly in the rates of storminess. Their effect has been indirect through changes in the low-frequency variations which then again have influenced storminess. In other words our findings show that there is a tendency to preserve the relation between low-frequency and high-frequency variations.

Appendix

Calculation of optimal predictor map

In the decomposition given by Eq. (1), there is a normalisation freedom. In our application we have normalised the PCs to unit standard deviation. That means that the variance (and units) are included in the EOFs. Introducing the inner-product notation for two spatial fields u and v given on grid points $i = 1, \ldots, N$ on a regular grid as

$$u, v = \sum_{i=1}^{N} u_i v_i w_i,$$

where w_i is a weight function varying as the reciprocal cosine to latitude to account for varying distance between grid points, the normalisation of the EOFs can be written as

$$\langle e_i, e_j \rangle = \sigma_i^2 \cdot \delta_{ij}.$$

The statistical regression model (2) can now be rewritten in non-dimensional form as

$$\frac{\chi - \bar{\chi}}{\sigma_\chi} = \frac{\sum_{i=1}^{4} b_i \alpha_i(t)}{(\sum_{i=1}^{4} b_i^2)^{1/2}} \tag{A1}$$

where $\bar{\chi}$ and σ_χ the mean and standard deviation of the predictand.

We want to define the *optimal predictor map* (OPM), given as a linear combination of the EOFs

$$\Psi = \sum_{i=1}^{4} c_i e_i \tag{A2}$$

and fulfilling the condition

$$\frac{\chi - \bar{\chi}}{\sigma_\chi} = \frac{1}{A} \langle \Psi, p' \rangle \tag{A3}$$

where A is a normalisation constant to be determined later.

Inserting the expansion (A2) into (A3) and comparing with (A1) we obtain

$$c_i = A \frac{1}{\sigma_i^2} \frac{b_i}{(\sum_{j=1}^{4} b_j^2)^{1/2}}, \; i = 1, \ldots, 4. \tag{A4}$$

Finally, we want to determine the coefficient A, so that an anomaly $p' = \Psi$ correspond to one standard deviation increase in the predictand, i.e. we want

$$\langle \Psi, \Psi \rangle = A. \tag{A5}$$

By inserting (A4) in (A2) and (A2) in (A5) one produces

$$A = \frac{\sum_{i=1}^{4} b_i^2}{\sum_{i=1}^{4} \left(\frac{b_i}{\sigma_j} \right)^2} \tag{A6}$$

and by combining (A6) and (A4) we obtain the final expression for the expansion coefficients

$$c_i = \frac{(\sum_{j=1}^{4} b_j^2)^{1/2}}{\sum_{j=1}^{4} \left(\frac{b_j}{\sigma_j} \right)^2} \frac{b_i}{\sigma_i^2}, \; i = 1, \ldots, 4. \tag{A7}$$

Acknowledgements This study was funded by the European Commission (Contract EV5V-CT94-0506). Our thanks to National Center for Atmospheric Research (NCAR), Boulder, Colorado, USA for providing the gridded MSL pressure dataset. The valuable discussions with our collegue Povl Frich are appreciated, as are the useful suggestions from the two reviewers.

References

Alexandersson H, Schmith T, Iden K, Tuomenvirta H (1997) Long-term variations of the storm climate over NW Europe. The Global Atmosphere and Ocean System, (accepted)

Berz G, Conrad K (1994) Stormy weather: the mounting windstorm risk and consequences for insurance industry (1994) Ecodesicion 12:65–69

Cardone V, Greenwood JG (1990) On trends in historical marine wind data. J Clim 3:113–127

Carnell RE, Senior CA, Mitchell JFB (1996) An assessment of measures of storminess: simulated changes in Northern Hemisphere winter due to increasing CO_2. Clim Dyn 12:467–476

Conrad V, Pollack C (1962) Methods in climatology. Harvard University Press, Cambridge, MA, USA

Greenpeace (1994) The climate time bomb. Greenpeace Council, Amsterdam, Netherlands
Hall NMJ, Hoskins BJ, Valdes PJ, Senior CA (1994) Storm tracks in high-resolution GCM with double carbon dioxide. QJR Meteorol. Soc 120 : 1209–1230
Hoskins BL, Valdes PJ (1990) On the existence of storm tracks. J Atmos Sci 47 : 1854–1864
Jenkins GM, Watts DG (1968) Spectral analysis and its applications. Holden-Day, San Francisco, CA, USA
Kaas E, Li T-S, Schmith T (1996) Statistical hindcast of wind climatology in the North Atlantic and northwestern European region. Clim Res 7(2) : 97–110
Lambert SJ (1996) Intense extratropical Northern Hemisphere winter cyclone events: 1899–1991. J Geo Res D 101 : 21319–21325
Lau N-C (1988) Variability of the observed midlatitude storm tracks in relation to low-frequency changes in the circulation pattern. J Atmos Sci 45 : 2718–2743
Lindzen RS, Farrell B (1980) A simple approximate result for maximum growth rate of baroclinic instabilities. J Atmos Sci 37 : 1648–1654
Lunkeit F, Ponater M, Sausen R, Sogalla M, Ulbrich U, Windelband M (1996) Cyclonic activity in a warmer climate. Contrib Atmos Phys 69(3) : 393–407
Rogers JC (1997) North Atlantic storm track variability and its association to the North Atlantic oscillation and climate variability of Northern Europe. J Clim 10 : 1635–1647
Schinke H (1993) On the occurrence of deep cyclones over Europe and the North Atlantic in the period 1930–1991. Contrib Atmos Phys 66(3): 223–237
Schmidt H, von Storch H (1993) German Bight storms analysed. Nature 370 : 791
Schmith T, Alexandersson H, Iden K, Tuomenvirta H (1997) North Atlantic-European pressure observations 1868–1995 (WASA dataset 1.0). Techn Rep 97–3, Danish Meteorological Institute, Copenhagen, Denmark
Stein O, Hense A (1994) A reconstructed time series of the number of extreme low pressure events since 1880 (1994) Meteorol Z NF3 : 43–46
von Storch H, Guddal J, Iden K, Jónsson T, Perlwitz J, Reistad M, de Ronde J, Schmidt H, Zorita E (1993) Changing statistics of storms in the North Atlantic? Report No. 116, Max-Planck-Institut für Meteorologie, Hamburg, Germany
Trenberth KE, Paolino Jr AD (1980) The northern hemisphere sea-level pressure data set: trends, errors and discontinuities. Mon Weather Rev 108 : 855–872
Walker GT, Bliss EW (1932) World weather V. Mem R Meteorol. Soc 4 : 53–84
Wallace JM, Lim G-H, Blackmon ML (1988) Relationship between cyclone tracks, anticyclone tracks and baroclinic waveguides. J Atmos Sci 45 : 439–462